Memorias del XVI Congreso Latinoamericano de Control Automático, CLCA 2014
Octubre 14-17, 2014. Cancún, Quintana Roo, México

Leader-Follower Consensus in Networks of Uncertain Manipulators in the $SE(3)$

Emmanuel Nuño [*], **Carlos Aldana** [**], **Luis Basañez** [**]

[*] *Department of Computer Science. CUCEI, University of Guadalajara. Guadalajara, Mexico.*
[**] *Institute of Industrial and Control Engineering, Technical University of Catalonia. Barcelona, Spain.*
emmanuel.nuno@cucei.udg.mx; {carlos.aldana; luis.basanez}@upc.edu

Abstract: This work presents a novel controller capable of solving the leader-follower consensus problem in networks of non-identical and kinematically different (heterogeneous) robot manipulators in the Special Euclidean space of dimension three, denoted $SE(3)$. The controller estimates the kinematic and the dynamic robot physical parameters and it is designed to be robust to interconnecting variable-time delays. Furthermore, the singularity-free unit-quaternions are employed to represent the orientation in the $SE(3)$. Simulations using a network with four 3-Degrees-of-Freedom manipulators illustrate the performance of the proposed controller.

Keywords: Robot networks, Adaptive Control, Time-Delays, Euler-Lagrange systems.

1. INTRODUCTION

In the $SE(3)$ space, the term pose is used to represent position and orientation (attitude). It is in this space where the robot tasks take place and the control in this space plays a major role in cooperative tasks performed by multiple robot manipulators primarily if they are kinematically and dynamically dissimilar (heterogeneous) (Liu and Chopra, 2012; Aldana et al., 2014). The practical applications of multi-robot systems span different areas such as underwater and space exploration, hazardous environments and service robotics.

This paper focusses on finding the solution to the leader-follower consensus problem in networks of heterogeneous robot manipulators with uncertain physical parameters and interconnecting variable time-delays. In the leader-follower consensus, the objective is to ensure that all manipulators converge to a given leader pose. The solutions to these problems have been widely studied for first and second-order *linear time invariant* systems (Olfati-Saber and Murray, 2004; Scardovi and Sepulchre, 2009; Ren, 2008). For *nonlinear* systems, the works of Liu and Chopra (2012); Rodriguez-Angeles and Nijmeijer (2004); Nuño et al. (2011); Wang (2013a) present a solution to the the leader-follower problem, provided that the leader position is available to *all* the agents. Mei et al. (2011) propose a sliding-based scheme for the leader-follower case assuming that the leader position and velocity is available only to a certain set of followers. Recently, Liu et al. (2014) have proposed a solution in the joint space and without interconnecting delays and Meng et al. (2014), using an adaptive sliding controller, solve the leader-follower synchronization in the joint space and without interconnecting delays.

This work is closely related to the insightful papers by Wang (2013a,b). Using similar kinematic and dynamic adaptation schemes as in (Cheah et al., 2006; Wang and Xie, 2009), on one hand, Wang (2013a) solves the leader-follower consensus provided that the leader position is available to *all* the agents and, on the other hand, Wang (2013b) solves the leaderless consensus problem without time-delays. Furthermore, for the orientation, these works make use of a minimal representation that exhibits singularities and it is assumed that all the agents are kinematically similar, i.e., all agents have the same degrees-of-freedom (DoF).

The *main contribution* of this work is a novel controller that solves the leader-follower consensus problem, with the following important features: 1) it is only assumed that there is at least one agent which can access the leader's pose; 2) the controller dynamically estimates all the uncertain physical parameters; 3) the controller is robust to interconnection variable time-delays and 4) for the orientation error, the controller makes use of unit-quaternions, which are a singularity free orientation representation. Furthermore, in order to show the performance of the proposed scheme, simulations using a network with four 3-DoF manipulators are also presented.

The following *notation* is used throughout the paper. $\mathbb{R} := (-\infty, \infty)$, $\mathbb{R}_{>0} := (0, \infty)$, $\mathbb{R}_{\geq 0} := [0, \infty)$. $|\mathbf{x}|$ stands for the standard Euclidean norm of vector $\mathbf{x}$. $\mathbf{I}_k$ represents the identity of size $k \times k$. $\mathbf{1}_k$ and $\mathbf{0}_k$ represent column vectors of size k with all entries equal to one and to zero, respectively. For any matrix $\mathbf{A} \in \mathbb{R}^{n \times m}$, $\mathbf{A}^\top(\mathbf{A}\mathbf{A}^\top)^{-1}$ is its Moore-Penrose pseudo-inverse matrix denoted by $\mathbf{A}^\dagger$. For any function $\mathbf{f} : \mathbb{R}_{\geq 0} \to \mathbb{R}^n$, the $\mathcal{L}_\infty$-norm is defined as $\|\mathbf{f}\|_\infty := \sup_{t \geq 0} |\mathbf{f}(t)|$, $\mathcal{L}_2$-norm as $\|\mathbf{f}\|_2 := (\int_0^\infty |\mathbf{f}(t)|^2 dt)^{1/2}$. The $\mathcal{L}_\infty$ and $\mathcal{L}_2$ spaces are defined as the sets $\{\mathbf{f} : \mathbb{R}_{\geq 0} \to \mathbb{R}^n | \ \|\mathbf{f}\|_\infty < \infty\}$ and $\{\mathbf{f} : \mathbb{R}_{\geq 0} \to \mathbb{R}^n | \ \|\mathbf{f}\|_2 < \infty\}$, respectively. The subscript $i \in \bar{N} := \{1, ..., N\}$, where N is the number of nodes of the network.

2. SYSTEM DYNAMICS

The dynamical behavior of the network accounts for a threefold: i) the dynamics of nodes; ii) the interconnection topology; and iii) the orientation description in the $SE(3)$.

2.1 Node Dynamics

The ith-node is modeled as n_i-DoF robot manipulator [1]. Its EL-equation of motion, in joint space, is given by

$$\mathbf{M}_i(\mathbf{q}_i)\ddot{\mathbf{q}}_i + \mathbf{C}_i(\mathbf{q}_i,\dot{\mathbf{q}}_i)\dot{\mathbf{q}}_i + \mathbf{g}_i(\mathbf{q}_i) = \boldsymbol{\tau}_i \tag{1}$$

where $\mathbf{q}_i, \dot{\mathbf{q}}_i, \ddot{\mathbf{q}}_i \in \mathbb{R}^{n_i}$, are the joint positions, velocities and accelerations, respectively; $\mathbf{M}_i(\mathbf{q}_i) \in \mathbb{R}^{n_i\times n_i}$ is the symmetric and positive definite inertia matrix; $\mathbf{C}_i(\mathbf{q}_i,\dot{\mathbf{q}}_i) \in \mathbb{R}^{n_i\times n_i}$ is the Coriolis and centrifugal effects matrix, defined via the Christoffel symbols of the first kind; $\mathbf{g}_i(\mathbf{q}_i) \in \mathbb{R}^{n_i}$ is the gravitational torques vector and $\boldsymbol{\tau}_i \in \mathbb{R}^{n_i}$ is the torque exerted by the actuators (motors).

The pose of the ith-end-effector, relative to a common reference frame, is denoted by the vector $\mathbf{x}_i \subset \mathbb{R}^7$ and it is composed of the position vector $\mathbf{p}_i \in \mathbb{R}^3$ and the orientation unit-quaternion [2] $\boldsymbol{\xi}_i \in S^3$, such that $\mathbf{x}_i := [\mathbf{p}_i^\top, \boldsymbol{\xi}_i^\top]^\top$. The kinematic relation between the joint velocities and the linear $\dot{\mathbf{p}}_i$ and angular $\boldsymbol{\omega}_i$ velocities of the ith-end-effectors relative to a common reference frame, is given by

$$\boldsymbol{\upsilon}_i = [\dot{\mathbf{p}}_i, \boldsymbol{\omega}_i]^\top = \mathbf{J}_i(\mathbf{q}_i)\dot{\mathbf{q}}_i \tag{2}$$

where $\boldsymbol{\upsilon}_i \in \mathbb{R}^6$ and $\mathbf{J}_i(\mathbf{q}_i) \in \mathbb{R}^{6\times n_i}$ is the *geometric Jacobian* matrix.

The EL-system (1) enjoys the following properties (Kelly et al., 2005; Spong et al., 2005):

- **P1**. For all $\mathbf{q}_i \in \mathbb{R}^{n_i}$, exist $\underline{M}_i, \bar{M}_i \in \mathbb{R}_{>0}$ such that $\underline{M}_i \leq \|\mathbf{M}_i(\mathbf{q}_i)\| \leq \bar{M}_i$.
- **P2**. Matrix $\dot{\mathbf{M}}_i(\mathbf{q}_i) - 2\mathbf{C}_i(\mathbf{q}_i,\dot{\mathbf{q}}_i)$ is skew-symmetric.
- **P3**. For any $\boldsymbol{\phi}_i \in \mathbb{R}^{n_i}$, (1) satisfies $\mathbf{M}_i(\mathbf{q}_i)\dot{\boldsymbol{\phi}}_i + \mathbf{C}_i(\mathbf{q}_i,\dot{\mathbf{q}}_i)\boldsymbol{\phi}_i - \mathbf{g}_i(\mathbf{q}_i) = \mathbf{Y}_{Di}(\mathbf{q}_i,\dot{\mathbf{q}}_i,\boldsymbol{\phi}_i,\dot{\boldsymbol{\phi}}_i)\boldsymbol{\theta}_{Di}$, where $\mathbf{Y}_{Di} \in \mathbb{R}^{n_i\times m_{Di}}$ is a regressor matrix of known functions and $\boldsymbol{\theta}_{Di} \in \mathbb{R}^{m_{Di}}$ is a constant vector containing the dynamical parameters (link masses, moments of inertia, etc.).
- **P4**. For all $\mathbf{q}_i \in \mathbb{R}^{n_i}$, the Jacobian matrix $\mathbf{J}_i(\mathbf{q}_i)$ is a bounded operator.
- **P5**. The kinematic relation (2) satisfies $\boldsymbol{\upsilon}_i = \mathbf{Y}_{Ki}(\mathbf{q}_i,\dot{\mathbf{q}}_i)\boldsymbol{\theta}_{Ki}$, where $\mathbf{Y}_{Ki} \in \mathbb{R}^{6\times m_{Ki}}$ is the kinematic regressor matrix and $\boldsymbol{\theta}_{Ki} \in \mathbb{R}^{m_{Ki}}$ is a constant vector containing the kinematic physical parameters (link lengths, center of mass distances, etc.).

2.2 Modeling the Interconnection

The interconnection of the N followers is modeled using the Laplacian matrix $\mathbf{L} := [\ell_{ij}] \in \mathbb{R}^{N\times N}$, whose elements are defined as

$$\ell_{ij} = \begin{cases} \sum_{j\in\mathcal{N}_i} w_{ij} & i = j \\ -w_{ij} & i \neq j \end{cases} \tag{3}$$

where $\mathcal{N}_i$ is the set of agents transmitting information to the ith robot, $w_{ij} > 0$ if $j \in \mathcal{N}_i$ and $w_{ij} = 0$ otherwise.

Similar to passivity-based (energy-shaping) synchronization (Nuño et al., 2013a; Arcak, 2007; Sarlette et al., 2009) and in order to ensure that the interconnection forces are generated by the gradient of a potential function, the following assumption is used in this paper:

- **A1**. The followers interconnection graph is *undirected and connected*.

By construction, $\mathbf{L}$ has a zero row sum, *i.e.*, $\mathbf{L}\mathbf{1}_N = \mathbf{0}_N$. Moreover, Assumption **A1**, ensures that $\mathbf{L}$ is symmetric, has a single zero-eigenvalue and the rest of the spectrum of $\mathbf{L}$ has positive real parts. Thus, $\text{rank}(\mathbf{L}) = N-1$. The Laplacian matrix models the followers interconnection and, in this work, we make use of a diagonal matrix $\mathbf{A} \in \mathbb{R}^{N\times N}$ to model the leader-follower interconnections. The following lemma, which is a special case of Lemma 1.6 by Cao and Ren (2011), provides an interesting property of the composed Laplacian matrix $\mathbf{L}_\ell := \mathbf{L} + \mathbf{A}$ that will be used in the proof of one of the main results.

Lemma 1. Consider a non-negative diagonal matrix $\mathbf{A} := \text{diag}(a_1,\ldots,a_N) \in \mathbb{R}^{N\times N}$ and suppose that, at least, one a_i is strictly positive, i.e., there exists some $a_i > 0$. Assume that **A1** holds, then the matrix $\mathbf{L}_\ell := \mathbf{L} + \mathbf{A}$ is symmetric, positive definite and of full rank. ◇

With regards to the interconnection time-delays, it is assumed that:

- **A2**. The information exchange, from the j-th agent to the i-th agent, is subject to a variable time-delay $T_{ji}(t)$ with a known upper-bound ${}^*T_{ji}$. Hence, it holds that $0 \leq T_{ji}(t) \leq {}^*T_{ji} < \infty$. Moreover, $\dot{T}_{ji}(t)$ is bounded.

2.3 Orientation in the SE(3)

Compared to other orientation representations, e.g., yaw-pitch-roll parameters, Euler angles, etc., the unit quaternions are known to be free of singularities (Caccavale et al., 1999). A unit-quaternion $\boldsymbol{\xi}_i \in S^3$ can be split in two elements: one scalar term $\eta_i \in \mathbb{R}$ and one vectorial term $\boldsymbol{\beta}_i \in \mathbb{R}^3$. Thus $\boldsymbol{\xi}_i := [\eta_i, \boldsymbol{\beta}_i^\top]^\top$ and, from the unit norm constraint, $\eta_i^2 + \boldsymbol{\beta}_i^\top\boldsymbol{\beta}_i = 1$ (refer to (Kuipers, 2002) for a detailed list of properties and operations involving unit-quaternions). The unit-quaternion $\boldsymbol{\xi}_i$ can be easily obtained from the direct kinematics function of each robot manipulator, via the rotation matrix $\mathbf{R}_i \in SO(3) := \{\mathbf{R}_i \in \mathbb{R}^{3\times 3} |\ \mathbf{R}_i^\top\mathbf{R}_i = \mathbf{I}_3, \det(\mathbf{R}_i) = 1\}$.

The orientation error, relative to the world frame, between two different frames, $\boldsymbol{\Sigma}_i$ and $\boldsymbol{\Sigma}_j$, can be described by the rotation matrix $\tilde{\mathbf{R}}_{ij} := \mathbf{R}_i\mathbf{R}_j^\top \in SO(3)$. The unit-quaternion describing such orientation error is given by

$$\tilde{\boldsymbol{\xi}}_{ij} = \boldsymbol{\xi}_i \odot \boldsymbol{\xi}_j^* = \begin{bmatrix} \eta_i\eta_j + \boldsymbol{\beta}_i^\top\boldsymbol{\beta}_j \\ -\mathbf{U}^\top(\boldsymbol{\xi}_i)\boldsymbol{\xi}_j \end{bmatrix} \tag{4}$$

where $\odot$ denotes the quaternion product, $\boldsymbol{\xi}_{(\cdot)}^* = [\eta_{(\cdot)}, -\boldsymbol{\beta}_{(\cdot)}^\top]^\top$ is the quaternion conjugate of $\boldsymbol{\xi}_{(\cdot)}$, $\mathbf{S}(\cdot)$ is the skew-symmetric matrix operator [3] and $\mathbf{U}(\boldsymbol{\xi}_i)$ is defined as

$$\mathbf{U}(\boldsymbol{\xi}_i) := \begin{bmatrix} -\boldsymbol{\beta}_i^\top \\ \eta_i\mathbf{I}_3 - \mathbf{S}(\boldsymbol{\beta}_i) \end{bmatrix}. \tag{5}$$

[1] Note that each robot may have different number of DoF.

[2] The set $S^3 \subset \mathbb{R}^4$ represents an unitary sphere of dimension three and it is defined as $S^3 := \{\boldsymbol{\xi} \in \mathbb{R}^4 |\ |\boldsymbol{\xi}|^2 = 1\}$.

[3] For any $\mathbf{a},\mathbf{b} \in \mathbb{R}^3$, $\mathbf{S}(\mathbf{a})\mathbf{b} = \mathbf{a}\times\mathbf{b}$. Some well known properties of the skew-symmetric matrix operator, $\mathbf{S}(\cdot)$, used throughout the paper, are: $\mathbf{S}(\mathbf{a})^\top = \mathbf{S}(-\mathbf{a}) = -\mathbf{S}(\mathbf{a})$ and $\mathbf{S}(\mathbf{a})\mathbf{a} = \mathbf{0}_3$.

The relation between the time-derivative of the unit-quaternion and the angular velocity, relative to the world reference frame, is given by

$$\dot{\boldsymbol{\xi}}_i = \frac{1}{2}\mathbf{U}(\boldsymbol{\xi}_i)\boldsymbol{\omega}_i. \tag{6}$$

Hence, defining $\boldsymbol{\Phi}(\boldsymbol{\xi}_i) := \text{diag}(\mathbf{I}_3, \frac{1}{2}\mathbf{U}(\boldsymbol{\xi}_i))$, it holds that

$$\dot{\mathbf{x}}_i = \boldsymbol{\Phi}(\boldsymbol{\xi}_i)\boldsymbol{\upsilon}_i. \tag{7}$$

The normality condition and some straightforward calculations show that $\tilde{\boldsymbol{\beta}}_{ij} = \mathbf{0}$ if and only if $\boldsymbol{\xi}_i = \pm\boldsymbol{\xi}_j$. This, in turn, implies that $\mathbf{U}^\top(\boldsymbol{\xi}_i)\boldsymbol{\xi}_j = \mathbf{0}_3$. A key observation is that $\boldsymbol{\xi}_i = \boldsymbol{\xi}_j$ and $\boldsymbol{\xi}_i = -\boldsymbol{\xi}_j$ represent the same physical orientation. The following properties have been borrowed from (Wen and Kreutz-Delgado, 1991; Fjellstad, 1994; Campa and Camarillo, 2008; Wang et al., 2012) and are used throughout the rest of the paper.

P6. For all $\boldsymbol{\xi}_i \in S^3$, $\mathbf{U}^\top(\boldsymbol{\xi}_i)\mathbf{U}(\boldsymbol{\xi}_i) = \mathbf{I}_3$. Hence, $\text{rank}(\mathbf{U}(\boldsymbol{\xi}_i)) = 3$ and $\ker(\mathbf{U}^\top(\boldsymbol{\xi}_i)) = \text{span}(\boldsymbol{\xi}_i)$.

P7. For all $\boldsymbol{\xi}_i \in S^3$ and $\dot{\boldsymbol{\xi}}_i \in \mathbb{R}^4$, $\dot{\mathbf{U}}(\boldsymbol{\xi}_i) = \mathbf{U}(\dot{\boldsymbol{\xi}}_i)$.

P8. Since, for all $\boldsymbol{\xi}_i \in S^3$, $|\boldsymbol{\xi}_i| = 1$ then $\mathbf{U}(\boldsymbol{\xi}_i)$ is a bounded operator.

3. CONSENSUS IN THE TASK SPACE

Consider a network of N equal or different EL-systems of the form (1). Assume that the interconnection graph fulfills Assumptions **A1** and **A2**. Furthermore, suppose that the kinematic and the dynamic physical parameters are uncertain. Under this scenario, in this paper is proposed a controller to solve the following consensus problem:

LFCP Leader-Follower Consensus Problem: The network of N followers has to be regulated at a given constant leader pose $\mathbf{x}_\ell := [\mathbf{p}_\ell^\top, \boldsymbol{\xi}_\ell^\top]^\top \subset \mathbb{R}^7$, provided that the leader pose is only available to a certain nonempty set of followers. Hence, for all $i \in \bar{N}$,

$$\lim_{t\to\infty} |\boldsymbol{\upsilon}_i(t)| = 0, \quad \lim_{t\to\infty} \mathbf{x}_i(t) = \mathbf{x}_\ell. \tag{8}$$

This paper makes the following assumption for the leader-follower interconnection:

A3. At least one of the N follower robots has direct access to the leader's pose $\mathbf{x}_\ell$.

Considering that the kinematic and the dynamic physical parameters are uncertain and using (2), together with **P3** and **P5**, it holds that

$$\hat{\mathbf{J}}_i(\mathbf{q}_i)\dot{\mathbf{q}}_i = \mathbf{Y}_{Ki}(\mathbf{q}_i, \dot{\mathbf{q}}_i)\hat{\boldsymbol{\theta}}_{Ki} \tag{9}$$

and

$\hat{\mathbf{M}}_i(\mathbf{q}_i)\dot{\boldsymbol{\phi}}_i + \hat{\mathbf{C}}_i(\mathbf{q}_i, \dot{\mathbf{q}}_i)\boldsymbol{\phi}_i - \hat{\mathbf{g}}_i(\mathbf{q}_i) = \mathbf{Y}_{Di}(\mathbf{q}_i, \dot{\mathbf{q}}_i, \boldsymbol{\phi}_i, \dot{\boldsymbol{\phi}}_i)\hat{\boldsymbol{\theta}}_{Di}$, where $\boldsymbol{\phi}_i \in \mathbb{R}^{n_i}$ is a differentiable signal that will be defined later, $\hat{\boldsymbol{\theta}}_{Ki} \in \mathbb{R}^{m_{Ki}}$ and $\hat{\boldsymbol{\theta}}_{Di} \in \mathbb{R}^{m_{Di}}$ are the kinematic and the dynamic estimated physical parameters, respectively. $\hat{\mathbf{J}}_i(\mathbf{q}_i), \hat{\mathbf{M}}_i(\mathbf{q}_i), \hat{\mathbf{C}}_i(\mathbf{q}_i, \dot{\mathbf{q}}_i)$ are the estimated Jacobian, inertia and Coriolis matrices and $\hat{\mathbf{g}}_i(\mathbf{q}_i)$ is the estimated gravity vector, all of them defined using the Jacobian, inertia, Coriolis and gravity terms evaluated using the estimated physical parameters.

Setting-up the controller

$$\boldsymbol{\tau}_i = -\mathbf{Y}_{Di}(\mathbf{q}_i, \dot{\mathbf{q}}_i, \boldsymbol{\phi}_i, \dot{\boldsymbol{\phi}}_i)\hat{\boldsymbol{\theta}}_{Di} - K_i\hat{\mathbf{J}}_i^\top(\mathbf{q}_i)\hat{\mathbf{J}}_i(\mathbf{q}_i)\boldsymbol{\epsilon}_i, \tag{10}$$

where $K_i \in \mathbb{R}_{>0}$ and

$$\boldsymbol{\epsilon}_i := \dot{\mathbf{q}}_i + \boldsymbol{\phi}_i, \tag{11}$$

yields the following closed-loop system

$$\mathbf{M}_i(\mathbf{q}_i)\dot{\boldsymbol{\epsilon}}_i + \mathbf{C}_i(\mathbf{q}_i, \dot{\mathbf{q}}_i)\boldsymbol{\epsilon}_i + K_i\hat{\mathbf{J}}_i^\top(\mathbf{q}_i)\hat{\mathbf{J}}_i(\mathbf{q}_i)\boldsymbol{\epsilon}_i = \mathbf{Y}_{Di}\tilde{\boldsymbol{\theta}}_{Di}, \tag{12}$$

with $\tilde{\boldsymbol{\theta}}_{Di} := \boldsymbol{\theta}_{Di} - \hat{\boldsymbol{\theta}}_{Di}$.

As usual in the *adaptive control* design, consider the energy-like function

$$\mathcal{V}_i = \frac{1}{2}\left[\boldsymbol{\epsilon}_i^\top\mathbf{M}_i(\mathbf{q}_i)\boldsymbol{\epsilon}_i + \tilde{\boldsymbol{\theta}}_{Di}^\top\boldsymbol{\Gamma}_{Di}^{-1}\tilde{\boldsymbol{\theta}}_{Di}\right],$$

where $\boldsymbol{\Gamma}_{Di} = \boldsymbol{\Gamma}_{Di}^\top > 0$. Evaluating $\dot{\mathcal{V}}_i$ along (12), using **P2**, the fact that $\dot{\tilde{\boldsymbol{\theta}}}_{Di} = -\dot{\hat{\boldsymbol{\theta}}}_{Di}$ and defining the parameter estimation law as

$$\dot{\hat{\boldsymbol{\theta}}}_{Di} := \boldsymbol{\Gamma}_{Di}\mathbf{Y}_{Di}^\top\boldsymbol{\epsilon}_i, \tag{13}$$

yields $\dot{\mathcal{V}}_i = -K_i|\hat{\mathbf{J}}_i(\mathbf{q}_i)\boldsymbol{\epsilon}_i|^2 \leq 0$.

Now, pre-multiplying (11) by $\hat{\mathbf{J}}_i(\mathbf{q}_i)$ and using (2) and (9) yields $\hat{\mathbf{J}}_i(\mathbf{q}_i)\boldsymbol{\epsilon}_i = \boldsymbol{\upsilon}_i + \hat{\mathbf{J}}_i(\mathbf{q}_i)\boldsymbol{\phi}_i + \mathbf{Y}_{Ki}(\mathbf{q}_i, \dot{\mathbf{q}}_i)\tilde{\boldsymbol{\theta}}_{Ki}$, where $\tilde{\boldsymbol{\theta}}_{Ki} = \hat{\boldsymbol{\theta}}_{Ki} - \boldsymbol{\theta}_{Ki}$. Hence, $\dot{\mathcal{V}}_i$ can be rewritten as

$$\begin{aligned}\dot{\mathcal{V}}_i = &- K_i\left[|\boldsymbol{\upsilon}_i + \hat{\mathbf{J}}_i(\mathbf{q}_i)\boldsymbol{\phi}_i|^2 + |\mathbf{Y}_{Ki}(\mathbf{q}_i, \dot{\mathbf{q}}_i)\tilde{\boldsymbol{\theta}}_{Ki}|^2\right] \\ &- 2K_i\tilde{\boldsymbol{\theta}}_{Ki}^\top\mathbf{Y}_{Ki}^\top(\mathbf{q}_i, \dot{\mathbf{q}}_i)\left[\boldsymbol{\upsilon}_i + \hat{\mathbf{J}}_i(\mathbf{q}_i)\boldsymbol{\phi}_i\right].\end{aligned}$$

The form of $\dot{\mathcal{V}}_i$ motivates us to propose the following function

$$\mathcal{W}_i = \frac{1}{K_i}\mathcal{V}_i + \tilde{\boldsymbol{\theta}}_{Ki}^\top\boldsymbol{\Gamma}_{Ki}^{-1}\tilde{\boldsymbol{\theta}}_{Ki}, \tag{14}$$

where $\boldsymbol{\Gamma}_{Ki} = \boldsymbol{\Gamma}_{Ki}^\top > 0$. Thus, setting the kinematic estimation parameter law as

$$\dot{\hat{\boldsymbol{\theta}}}_{Ki} := \boldsymbol{\Gamma}_{Ki}\mathbf{Y}_{Ki}^\top(\mathbf{q}_i, \dot{\mathbf{q}}_i)\left[\boldsymbol{\upsilon}_i + \hat{\mathbf{J}}_i(\mathbf{q}_i)\boldsymbol{\phi}_i\right], \tag{15}$$

ensures that

$$\dot{\mathcal{W}}_i = -|\boldsymbol{\upsilon}_i|^2 - 2\boldsymbol{\upsilon}_i^\top\hat{\mathbf{J}}_i(\mathbf{q}_i)\boldsymbol{\phi}_i - |\hat{\mathbf{J}}_i(\mathbf{q}_i)\boldsymbol{\phi}_i|^2 - |\mathbf{Y}_{Ki}(\mathbf{q}_i, \dot{\mathbf{q}}_i)\tilde{\boldsymbol{\theta}}_{Ki}|^2.$$

Since $\boldsymbol{\upsilon}_i$ is the linear and angular velocities vector, the crossed term $\boldsymbol{\upsilon}_i^\top\hat{\mathbf{J}}_i(\mathbf{q}_i)\boldsymbol{\phi}_i$ in the last equation, suggests the design of $\boldsymbol{\phi}_i$ as a function of the pose error. Hence, let us define

$$\boldsymbol{\phi}_i := \hat{\mathbf{J}}_i^\dagger(\mathbf{q}_i)\boldsymbol{\Phi}^\top(\boldsymbol{\xi}_i)\mathbf{e}_i \tag{16}$$

where $\mathbf{e}_i$ is the pose error, between each manipulator with its leader and its neighbors, given by

$$\mathbf{e}_i := a_i(\mathbf{x}_i - \mathbf{x}_\ell) + \sum_{j\in\mathcal{N}_i} w_{ij}\left[\mathbf{x}_i - \mathbf{x}_j(t - T_{ji}(t))\right], \tag{17}$$

where $a_i > 0$ if the leader's pose $\mathbf{x}_\ell$ is available to the ith manipulator and $a_i = 0$, otherwise.

Let us propose the total energy-like function $\mathcal{H}_i$ as

$$\mathcal{H}_i = \mathcal{W}_i + a_i|\mathbf{x}_i - \mathbf{x}_\ell|^2 + \frac{1}{2}\sum_{j\in\mathcal{N}_i} w_{ij}|\mathbf{x}_i - \mathbf{x}_j|^2. \tag{18}$$

After some simple algebraic manipulations and using (17), $\dot{\mathcal{H}}_i$ is given by

$$\begin{aligned}\dot{\mathcal{H}}_i = &- |\boldsymbol{\upsilon}_i|^2 - |\boldsymbol{\Phi}^\top(\boldsymbol{\xi}_i)\mathbf{e}_i|^2 - \sum_{j\in\mathcal{N}_i} w_{ij}(\dot{\mathbf{x}}_i + \dot{\mathbf{x}}_j)^\top(\mathbf{x}_i - \mathbf{x}_j) \\ &- |\mathbf{Y}_{Ki}\tilde{\boldsymbol{\theta}}_{Ki}|^2 - 2\sum_{j\in\mathcal{N}_i} w_{ij}\dot{\mathbf{x}}_i^\top\int_{t-T_{ji}(t)}^{t}\dot{\mathbf{x}}_j(\sigma)d\sigma,\end{aligned}$$

where, to obtain the last expression, the transformation $\int_{t-T_{ji}(t)}^{t}\dot{\mathbf{x}}_j(\sigma)d\sigma = \mathbf{x}_j - \mathbf{x}_j(t - T_{ji}(t))$ has been used.

Following a similar procedure as in the proof of Proposition 1 in (Nuño et al., 2013b), defining $\mathbf{Q} := [\mathbf{x}_1^\top\dot{\mathbf{x}}_1, \ldots, \mathbf{x}_N^\top\dot{\mathbf{x}}_N]^\top$,

using (3) and since $\sum_{i\in\bar{N}}\sum_{j\in\mathcal{N}_i} w_{ij}(Q_i - Q_j) = \mathbf{1}_N^\top \mathbf{L}\mathbf{Q} = 0$, it is straightforward to show that, for $\mathcal{H} = \sum_{i\in\bar{N}} \mathcal{H}_i$,

$$\dot{\mathcal{H}} = -\sum_{i\in\bar{N}} \left[|\dot{\mathbf{x}}_i|^2 + 3|\dot{\boldsymbol{\xi}}_i|^2 + |\boldsymbol{\Phi}^\top(\boldsymbol{\xi}_i)\mathbf{e}_i|^2 + |\mathbf{Y}_{Ki}\tilde{\boldsymbol{\theta}}_{Ki}|^2\right] - 2\sum_{i\in\bar{N}}\sum_{j\in\mathcal{N}_i} w_{ij}\dot{\mathbf{x}}_i^\top \int_{t-T_{ji}(t)}^{t} \dot{\mathbf{x}}_j(\sigma)d\sigma.$$

Note that $\mathcal{H}$ does not qualify as a Lyapunov Function, i.e., it does not satisfy $\dot{\mathcal{H}} < 0$. Then, in the same spirit as in (Nuño et al., 2013b), and in order to get the below inequality, we integrate $\dot{\mathcal{H}}$ from 0 to t and apply Lemma 1 of (Nuño et al., 2009) to the double integral terms with $\alpha_i \in \mathbb{R}_{>0}$. This yields

$$\mathcal{H}(0) \geq \mathcal{H}(t) + \sum_{i\in\bar{N}} \left(\|\boldsymbol{\Phi}^\top(\boldsymbol{\xi}_i)\mathbf{e}_i\|_2^2 + \|\mathbf{Y}_{Ki}\tilde{\boldsymbol{\theta}}_{Ki}\|_2^2\right) + \sum_{i\in\bar{N}}\sum_{j\in\mathcal{N}_i} w_{ij}\left[\left(\frac{1}{\ell_{ii}} - \alpha_i\right)\|\dot{\mathbf{x}}_i\|_2^2 - \frac{{}^*T_{ji}^2}{\alpha_i}\|\dot{\mathbf{x}}_j\|_2^2\right],$$

where the fact that $\ell_{ii} := \sum_{j\in\mathcal{N}_i} w_{ij}$ has also been used. Defining the matrix $\boldsymbol{\Psi} \in \mathbb{R}^{N\times N}$ as

$$\boldsymbol{\Psi} := \begin{bmatrix} 1-\ell_{11}\alpha_1 & -\frac{w_{12}{}^*T_{21}^2}{\alpha_1} & \cdots & -\frac{w_{1N}{}^*T_{N1}^2}{\alpha_1} \\ -\frac{w_{12}{}^*T_{12}^2}{\alpha_2} & 1-\ell_{22}\alpha_2 & \cdots & -\frac{w_{2N}{}^*T_{N2}^2}{\alpha_2} \\ \vdots & \vdots & \ddots & \vdots \\ -\frac{w_{1N}{}^*T_{1N}^2}{\alpha_N} & -\frac{w_{2N}{}^*T_{2N}^2}{\alpha_N} & \cdots & 1-\ell_{NN}\alpha_N \end{bmatrix},$$

yields $\mathcal{H}(0) \geq \mathcal{H}(t) + \sum_{i\in\bar{N}} \left(\|\boldsymbol{\Phi}^\top(\boldsymbol{\xi}_i)\mathbf{e}_i\|_2^2 + \|\mathbf{Y}_{Ki}\tilde{\boldsymbol{\theta}}_{Ki}\|_2^2\right) + \mathbf{1}_N^\top\boldsymbol{\Psi}\left[\|\dot{\mathbf{x}}_1\|_2^2, \ldots, \|\dot{\mathbf{x}}_N\|_2^2\right]^\top$.

Setting α_i and weights w_{ij}, such that

$$1 > \sum_{j\in\mathcal{N}_i} w_{ij}\left(\alpha_i + \frac{{}^*T_{ij}^2}{\alpha_j}\right), \tag{19}$$

then there exists $\boldsymbol{\mu} \in \mathbb{R}^N$, defined as $\boldsymbol{\mu} := \boldsymbol{\Psi}^\top\mathbf{1}_N$, such that $\mu_i > 0$, for all $i \in \bar{N}$. Hence
$\mathcal{H}(0) \geq \mathcal{H}(t) + \sum_{i\in\bar{N}} \left(\|\boldsymbol{\Phi}^\top(\boldsymbol{\xi}_i)\mathbf{e}_i\|_2^2 + \|\mathbf{Y}_{Ki}\tilde{\boldsymbol{\theta}}_{Ki}\|_2^2 + \mu_i\|\dot{\mathbf{x}}_i\|_2^2\right)$.
Since $\mathcal{H}(0)$ is a positive constant and $\mathcal{H}(t) > 0$, then $\boldsymbol{\Phi}^\top(\boldsymbol{\xi}_i)\mathbf{e}_i, \mathbf{Y}_{Ki}\tilde{\boldsymbol{\theta}}_{Ki}, \dot{\mathbf{x}}_i \in \mathcal{L}_2$ and $\mathcal{H} \in \mathcal{L}_\infty$. Furthermore, $\mathcal{H}$ is positive definite and radially unbounded with regards to $\boldsymbol{\epsilon}_i, \tilde{\boldsymbol{\theta}}_{Di}, \tilde{\boldsymbol{\theta}}_{Ki}, |\mathbf{x}_i - \mathbf{x}_\ell|, |\mathbf{x}_i - \mathbf{x}_j|$, hence $\mathcal{H} \in \mathcal{L}_\infty$ ensures that all these signals are also bounded.

On one hand, **P8**, $\dot{\mathbf{x}}_i \in \mathcal{L}_2$ and $\tilde{\boldsymbol{\theta}}_{Ki}, |\mathbf{x}_i - \mathbf{x}_\ell|, |\mathbf{x}_i - \mathbf{x}_j| \in \mathcal{L}_\infty$, for all $i \in \bar{N}$ and $j \in \mathcal{N}_i$, together with **P4** imply that $\boldsymbol{\Phi}^\top(\boldsymbol{\xi}_i)\mathbf{e}_i, \boldsymbol{\phi}_i \in \mathcal{L}_\infty$. On the other hand, $\boldsymbol{\epsilon}_i, \boldsymbol{\phi}_i \in \mathcal{L}_\infty$ ensures that $\dot{\mathbf{q}}_i \in \mathcal{L}_\infty$, which together with **P4** and **P8**, implies that $\dot{\mathbf{x}}_i \in \mathcal{L}_\infty$.

Using (17) and boundedness of $\dot{\mathbf{x}}_i$ and **A2** support the fact that $\dot{\mathbf{e}}_i$ is also bounded. Furthermore, $\dot{\boldsymbol{\phi}}_i$ satisfies

$$\dot{\boldsymbol{\phi}}_i = \dot{\hat{\mathbf{J}}}_i^\dagger(\mathbf{q}_i)\boldsymbol{\Phi}^\top(\boldsymbol{\xi}_i)\mathbf{e}_i + \hat{\mathbf{J}}_i^\dagger(\mathbf{q}_i)\left[\dot{\boldsymbol{\Phi}}^\top(\boldsymbol{\xi}_i)\mathbf{e}_i + \boldsymbol{\Phi}^\top(\boldsymbol{\xi}_i)\dot{\mathbf{e}}_i\right]. \tag{20}$$

Hence assumption **A2**, properties **P4** and **P8** and boundedness of $\dot{\mathbf{q}}_i, \dot{\mathbf{x}}_i$ and $\dot{\mathbf{e}}_i$ imply that $\dot{\boldsymbol{\phi}}_i \in \mathcal{L}_\infty$ and, consequently, $\frac{d}{dt}\left(\boldsymbol{\Phi}^\top(\boldsymbol{\xi}_i)\mathbf{e}_i\right) \in \mathcal{L}_\infty$.

Now, boundedness of all these signals ensure, from the closed-loop system (12), that $\dot{\boldsymbol{\epsilon}}_i \in \mathcal{L}_\infty$. Since $\dot{\boldsymbol{\epsilon}}_i = \ddot{\mathbf{q}}_i + \dot{\boldsymbol{\phi}}_i$, $\ddot{\mathbf{q}}_i \in \mathcal{L}_\infty$. Furthermore,
$\ddot{\mathbf{x}}_i = \boldsymbol{\Phi}^\top(\boldsymbol{\xi}_i)\left[\mathbf{J}_i(\mathbf{q}_i)\ddot{\mathbf{q}}_i + \dot{\mathbf{J}}_i(\mathbf{q}_i)\dot{\mathbf{q}}_i\right] + \dot{\boldsymbol{\Phi}}^\top(\boldsymbol{\xi}_i)\mathbf{J}_i(\mathbf{q}_i)\dot{\mathbf{q}}_i$,
thus **P4**, **P8** and $\dot{\mathbf{x}}_i, \dot{\mathbf{q}}_i, \ddot{\mathbf{q}}_i \in \mathcal{L}_\infty$ ensure that $\ddot{\mathbf{x}}_i \in \mathcal{L}_\infty$. Finally, $\boldsymbol{\Phi}^\top(\boldsymbol{\xi}_i)\mathbf{e}_i, \dot{\mathbf{x}}_i \in \mathcal{L}_2 \cap \mathcal{L}_\infty$ and $\frac{d}{dt}\left(\boldsymbol{\Phi}^\top(\boldsymbol{\xi}_i)\mathbf{e}_i\right), \ddot{\mathbf{x}}_i \in \mathcal{L}_\infty$ yields, by Barbălat's Lemma, $\lim_{t\to\infty}|\boldsymbol{\Phi}^\top(\boldsymbol{\xi}_i(t))\mathbf{e}_i(t)| = 0$, $\lim_{t\to\infty}|\dot{\mathbf{x}}_i(t)| = 0$ and, from **P6**, $\lim_{t\to\infty}|\boldsymbol{\upsilon}_i(t)| = 0$.

Before presenting the main result, it should be mentioned that, although $\boldsymbol{\xi}_i = \boldsymbol{\xi}_\ell$ and $\boldsymbol{\xi}_i = -\boldsymbol{\xi}_\ell$ represent the same physical orientation, the closed-loop system (12) has two possible equilibria. However, $\boldsymbol{\xi}_i = -\boldsymbol{\xi}_\ell$ corresponds to an unstable equilibrium point.

Proposition 1. Suppose that Assumptions **A1**, **A2** and **A3** hold. Additionally assume that, for any $\alpha_i > 0$, condition (19) holds. Then, the controller given by (10), (11), (16) and (20) together with the dynamic and kinematic parameter estimation laws (13) and (15), respectively, solves the **LFCP** everywhere except when $(\dot{\mathbf{x}}_i(0), \mathbf{p}_i(0), \boldsymbol{\xi}_i(0)) = (\mathbf{0}_7, \mathbf{p}_\ell, -\boldsymbol{\xi}_\ell)$ for all $i \in \bar{N}$. ◇

Proof. First note that $\lim_{t\to\infty}|\dot{\mathbf{x}}_i(t)| = 0$ implies that $\int_{t-T_{ji}(t)}^{t}\dot{\mathbf{x}}_j(\sigma)d\sigma = \mathbf{x}_j - \mathbf{x}_j(t - T_{ji}(t)) = \mathbf{0}_7$. This and $\boldsymbol{\Phi}^\top(\boldsymbol{\xi}_i)\mathbf{e}_i = \mathbf{0}_6$ ensure that
$a_i(\mathbf{p}_i - \mathbf{p}_\ell) + \sum_{j\in\mathcal{N}_i} w_{ij}(\mathbf{p}_i - \mathbf{p}_j) = \mathbf{0}_3$
and
$a_i\mathbf{U}^\top(\boldsymbol{\xi}_i)(\boldsymbol{\xi}_i - \boldsymbol{\xi}_\ell) + \sum_{j\in\mathcal{N}_i} w_{ij}\mathbf{U}^\top(\boldsymbol{\xi}_i)(\boldsymbol{\xi}_i - \boldsymbol{\xi}_j) = \mathbf{0}_3$.

On one hand, defining $\mathbf{p} := [\mathbf{p}_1^\top, \ldots, \mathbf{p}_N^\top]^\top$ allows to rewrite the position error as $(\mathbf{A}\otimes\mathbf{I}_3)(\mathbf{p} - (\mathbf{1}_N\otimes\mathbf{p}_\ell)) + (\mathbf{L}\otimes\mathbf{I}_3)\mathbf{p} = \mathbf{0}_{3N}$ and, with the fact that $\mathbf{L}\mathbf{1}_N = \mathbf{0}_N$, yields $(\mathbf{L}_\ell\otimes\mathbf{I}_3)(\mathbf{p} - (\mathbf{1}_N\otimes\mathbf{p}_\ell)) = \mathbf{0}_{3N}$, where $\mathbf{A}$ and $\mathbf{L}_\ell$ are defined in Proposition 1. Further, Proposition 1 and the Kronecker product properties ensure that $\text{rank}(\mathbf{L}_\ell\otimes\mathbf{I}_3) = 3N$. Thus, $\mathbf{p}_i = \mathbf{p}_\ell$ is the only solution to the error equation.

On the other hand, defining $\boldsymbol{\xi} := [\boldsymbol{\xi}_1^\top, \ldots, \boldsymbol{\xi}_N^\top]^\top$ and $\bar{\mathbf{U}} := \text{diag}(\mathbf{U}(\boldsymbol{\xi}_1), \ldots, \mathbf{U}(\boldsymbol{\xi}_N)) \in \mathbb{R}^{4N\times 3N}$, the orientation error can be written as
$\bar{\mathbf{U}}^\top(\mathbf{A}\otimes\mathbf{I}_4)(\boldsymbol{\xi} - (\mathbf{1}_N\otimes\boldsymbol{\xi}_\ell)) + \bar{\mathbf{U}}^\top(\mathbf{L}\otimes\mathbf{I}_3)(\boldsymbol{\xi} - (\mathbf{1}_N\otimes\boldsymbol{\xi}_\ell)) = \mathbf{0}_{3N}$
or, what is the same, $\bar{\mathbf{U}}^\top(\mathbf{L}_\ell\otimes\mathbf{I}_4)(\boldsymbol{\xi} - (\mathbf{1}_N\otimes\boldsymbol{\xi}_\ell)) = \mathbf{0}_{3N}$. Since $(\mathbf{L}_\ell\otimes\mathbf{I}_4)$ is of full rank then $\boldsymbol{\xi} = (\mathbf{1}_N\otimes\boldsymbol{\xi}_\ell)$ is the only solution to $(\mathbf{L}_\ell\otimes\mathbf{I}_4)(\boldsymbol{\xi} - (\mathbf{1}_N\otimes\boldsymbol{\xi}_\ell)) = \mathbf{0}_{3N}$ and thus it satisfies this equation. However, the fact that $\text{rank}(\bar{\mathbf{U}}) = 3N$ and **P6** ensure that $\boldsymbol{\xi}_i = \pm\boldsymbol{\xi}_\ell$ are the only two solutions to the orientation error equation.

Using (18) it can be shown that $\boldsymbol{\xi}_i = \boldsymbol{\xi}_\ell$ corresponds to a minimum energy point and, since $\mathcal{H}(t)$ is a decreasing function, *i.e.*, $\mathcal{H}(0) \geq \mathcal{H}(t)$ for all $t \geq 0$, any perturbation from the other equilibrium point $\boldsymbol{\xi}_i = -\boldsymbol{\xi}_\ell$ will drive the system to $\boldsymbol{\xi}_i = \boldsymbol{\xi}_\ell$. Hence, $(\boldsymbol{\upsilon}_i, \mathbf{p}_i, \boldsymbol{\xi}_i) = (\mathbf{0}_6, \mathbf{p}_\ell, \boldsymbol{\xi}_\ell)$ is asymptotically stable everywhere except at the unstable equilibrium point $(\boldsymbol{\upsilon}_i, \mathbf{p}_i, \boldsymbol{\xi}_i) = (\mathbf{0}_6, \mathbf{p}_\ell, -\boldsymbol{\xi}_\ell)$. □

4. SIMULATIONS

This section provides simulation results that demonstrate the effectiveness of the proposed consensus algorithms, which are composed of four 3-DoF robot manipulators. The simulations have been carried on using Matlab's Simulink version 8.1. The unit-quaternions are derived from the rotation matrix following the algorithm proposed in (Spurrier, 1978). Each element of the ith kinematic regressor $\mathbf{Y}_{Ki}(\mathbf{q}_i, \dot{\mathbf{q}}_i) = [y_{kj,i}]$ is given by $y_{11,i} = -\dot{q}_{1,i}S_{i,1}$; $y_{12,i} = -(\dot{q}_{1,i}+\dot{q}_{2,i})S_{i,1+2}$; $y_{13,i} = -(\dot{q}_{1,i}+\dot{q}_{2,i}+\dot{q}_{3,i})S_{i,1+2+3}$; $y_{21,i} = \dot{q}_{1,i}C_{i,1}$; $y_{22,i} = (\dot{q}_{1,i}+\dot{q}_{2,i})C_{i,1+2}$; $y_{23,i} = (\dot{q}_{1,i}+\dot{q}_{2,i}+\dot{q}_{3,i})C_{i,1+2+3}$; $y_{24,i} = y_{14,i} = y_{31,i} = y_{32,i} = y_{33,i} = y_{34,i} = y_{41,i} = y_{42,i} = y_{43,i} = y_{44,i} = y_{51,i} = y_{52,i} = y_{53,i} = y_{53,i} = y_{61,i} = y_{62,i} = y_{63,i} = 0$ and $y_{64,i} = \dot{q}_{1,i} + \dot{q}_{2,i} + \dot{q}_{3,i}$, where the notation $C_{i,1+\ldots+n}$ and $S_{i,1+\ldots+n}$ are abbreviations for $\cos(q_{1,i}+\ldots+q_{n,i})$ and $\sin(q_{1,i}+\ldots+q_{n,i})$, respectively. The kinematic parameter vector is defined as $\boldsymbol{\theta}_{Ki} = [l_{1,i}, l_{2,i}, l_{3,i}, 1]$. The four manipulators have different physical parameters, these are shown in Table 1. The initial conditions for the estimated kinematic parameters are: $\hat{\theta}_{K1}(0) = \hat{\theta}_{K2}(0) = [0.50, 0.65, 0.40, 0.9]^\top$, $\hat{\theta}_{K3}(0) = [0.60, 0.67, 0.45, 0.9]^\top$ and $\hat{\theta}_{K4}(0) = [0.35, 0.60, 0.35, 0.9]^\top$.

The nonlinear dynamic model and the dynamic regressors of the 3-DoF robot are omitted for brevity. The initial estimated dynamic parameters are set to zero. The variable time-delays between the nodes are given by $T_{ji} = \rho + a_1 sin(\vartheta_1 t) + a_2 sin(\vartheta_2 t)$. Table 2 lists the values of the delays parameters.

Table 1. Robot 3-DoF and robots physical parameters.

Robot 3-DoF	Mass(kg) Inertia(kgm^2)	Length(m) C. of mass(m)
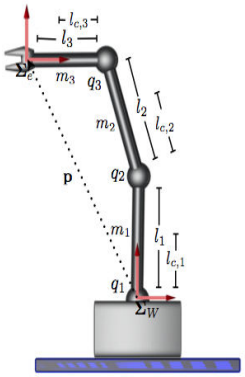	Robot 1 and 2 m_1=2 m_2=2 m_3=1.5 I_1=0.5 I_2=0.5 I_3=0.25 Robot 3 m_1=2.45 m_2=2.30 m_3=1.825 I_1=0.63 I_2=0.60 I_3=0.29 Robot 4 m_1=1.8 m_2=1.7 m_3=1.1 I_1=0.465 I_2=0.450 I_3=0.220	Robot 1 and 2 l_1=0.80 l_2=0.80 l_3=0.65 lc_1=0.40 lc_2=0.40 lc_3=0.325 Robot 3 l_1=0.82 l_2=0.74 l_3=0.58 lc_1=0.41 lc_2=0.37 lc_3=0.29 Robot 4 l_1=0.90 l_2=0.85 l_3=0.67 lc_1=0.45 lc_2=0.425 lc_3=0.335

The controller gains employed in this simulation are $K_1 = K_2 = K_3 = 480$, $K_4 = 550$, $\boldsymbol{\Gamma}_{Di} = 1700\mathbf{I}_9$, and $\boldsymbol{\Gamma}_{Ki} = 1700\mathbf{I}_4$ for $i \in \{1, 2, 3, 4\}$. For this case, only Node 4 receives the leader constant pose $\mathbf{x}_\ell = [0.98, 1.45, 0, 0.7163, 0, 0, 0.6978]^\top$ with an interconnection weight set to $a_4 = 5$. The follower interconnection weights are: $w_{12} = w_{21} = 1.5, w_{13} = w_{31} = .8, w_{23} = w_{32} = .7$ and $w_{34} = w_{43} = .8$, these weights fulfil (19) using

Table 2. Parameters of the variable time-delays.

Delay	ρ	a_1	ϑ_1(rad/s)	a_2	$\vartheta_2(rad/s)$
T_{21}	0.12	0.05	7	0.06	27
T_{31}	0.09	0.03	2	0.05	14
T_{12}	0.14	0.03	5	0.08	23
T_{32}	0.14	0.06	2	0.08	13
T_{13}	0.11	0.04	3	0.07	27
T_{23}	0.08	0.03	8	0.05	18
T_{43}	0.13	0.05	4	0.07	29
T_{34}	0.11	0.05	6	0.06	30

α_1=0.217, α_2=0.259, α_3=0.279, and α_4=.990. Figures 1 and 2 show the position and the quaternion orientation dynamic behavior for the leader-follower control algorithm. It is observed that despite the time-delays and the differences in the robots initial conditions, the robots asymptotically converge to the leader pose. Fig. 3 depicts the kinematic parameter estimation for each robot manipulator.

5. CONCLUSIONS

This paper proposes a novel adaptive controller that is capable of solving the leader-follower consensus problem in networks of heterogeneous robot manipulators in the task space. The controller only requires that the leader pose be available to, at least, one follower. Moreover, the controller is robust to parameter uncertainty and to variable time-delays in the interconnection. Furthermore, the orientation of the robot end-effectors is represented by the singularity-free unit-quaternions. Simulations, using a network with four manipulators, are shown to illustrate the performance of the proposed scheme.

ACKNOWLEDGEMENTS

This work has been partially supported by the Mexican CONACyT projects CB-129079 and and INFR-229696 and by the Spanish CICYT projects DPI2010-15446 and DPI2011-22471. The second author gratefully acknowledges the Mexican CONACyT for the doctoral grant 168998.

REFERENCES

C.I. Aldana, E Nuño, L. Basañez, and E. Romero. Operational space consensus of multiple heterogeneous robots without velocity measurements. *Journal of the Franklin Institute*, 351(3):1517–1539, 2014.

M. Arcak. Passivity as a design tool for group coordination. *IEEE T. Autom. Control*, 52(8):1380–1390, 2007.

F. Caccavale, B. Siciliano, and L. Villani. The role of Euler parameters in robot control. *Asian J. Control*, 1(1):25–34, 1999.

R. Campa and K. Camarillo. *Robot manipulators*, chapter Unit quaternions: A mathematical tool for modeling, path planning and control of robot manipulators, pages 21–48. InTech, 2008.

Y. Cao and W. Ren. *Distributed Coordination of Multi-agent Networks: Emergent Problems, Models, and Issues*. Springer-Verlag, 2011.

C.C. Cheah, C. Liu, and J.-J. Slotine. Adaptive jacobian tracking control of robots with uncertainties in kinematic, dynamic and actuator models. *IEEE Transactions on Automatic Control*, 51(6):1024–1029, 2006.

O.E. Fjellstad. *Control of unmanned underwater vehicles in six degrees of freedom: a quaternion feedback approach*. PhD thesis, Norwegian Institute of Technology, University of Trondheim, 1994.

R. Kelly, V. Santibáñez, and A. Loria. *Control of robot manipulators in joint space*. Springer-Verlag, 2005.

J. B. Kuipers. *Quaternions and Rotation Sequences: A Primer with Applications to Orbits, Aerospace and Virtual Reality*. Princeton University Press, 2002.

Y. Liu, H. Min, S. Wang, Z. Liu, and S. Liao. Distributed consensus of a class of networked heterogeneous multi-agent systems. *Journal of the Franklin Institute*, 351(3): 1700–1716, 2014.

Y.C. Liu and N. Chopra. Controlled synchronization of heterogeneous robotic manipulators in the task space. *IEEE Trans. Robot.*, 28(1):268–275, feb. 2012.

J. Mei, W. Ren, and G. Ma. Distributed coordinated tracking with a dynamic leader for multiple Euler-Lagrange systems. *IEEE Trans. Autom. Control*, 56(6): 1415–1421, June 2011.

Z. Meng, D.V. Dimarogonas, and K.H. Johansson. Leader-follower coordinated tracking of multiple heterogeneous lagrange systems using continuous control. *IEEE Trans. Robot. DOI: 10.1109/TRO.2013.2294060*, 2014.

E. Nuño, L. Basañez, R. Ortega, and M.W. Spong. Position tracking for nonlinear teleoperators with variable time-delay. *Int. J. Robot. Res.*, 28(7):895–910, 2009.

E. Nuño, R. Ortega, L. Basañez, and D. Hill. Synchronization of networks of nonidentical Euler-Lagrange systems with uncertain parameters and communication delays. *IEEE Trans. Autom. Control*, 56(4):935–941, 2011.

E. Nuño, R. Ortega, B. Jayawardhana, and L. Basañez. Coordination of multi-agent Euler-Lagrange systems via energy-shaping: Networking improves robustness. *Automatica*, 49(10):3065–3071, 2013a.

E. Nuño, I. Sarras, and L. Basañez. Consensus in networks of nonidentical Euler-Lagrange systems using P+d controllers. *IEEE T. Robot.*, 26(6):1503–1508, 2013b.

R. Olfati-Saber and R.M. Murray. Consensus problems in networks of agents with switching topology and time-delays. *IEEE T. Auto. Control*, 49(9):1520–1533, 2004.

W. Ren. On consensus algorithms for double-integrator dynamics. *IEEE T. Auto. Contr.*, 53(6):1503–150, 2008.

A. Rodriguez-Angeles and H. Nijmeijer. Mutual synchronization of robots via estimated state feedback: A cooperative approach. *IEEE Trans. Control Syst. Technol.*, 12(4):542–554, July 2004.

A. Sarlette, R. Sepulchre, and N.E. Leonard. Autonomous rigid body attitude synchronization. *Automatica*, 45(2): 572–577, 2009.

L. Scardovi and R. Sepulchre. Synchronization in networks of identical linear systems. *Automatica*, 45(11):2557–2562, 2009.

M.W. Spong, S. Hutchinson, and M. Vidyasagar. *Robot Modeling and Control*. Wiley, 2005.

R. A. Spurrier. Comment on singularity-free extraction of a quaternion from a direction-cosine matrix. *J. Spacecraft and Rockets*, 15(4):255, 1978.

H. Wang. Passivity based synchronization for networked robotic systems with uncertain kinematics and dynamics. *Automatica*, 49(3):755–761, 2013a.

H. Wang. Task-space synchronization of networked robotic systems with uncertain kinematics and dynamics. *IEEE Transactions on Automatic Control*, doi: 10.1109/TAC.2013.2254001:1–6, 2013b.

H. Wang and Y. Xie. Adaptive inverse dynamics control of robots with uncertain kinematics and dynamics. *Automatica*, 45(9):2114–2119, 2009.

X. Wang, C. Yu, and Z. Lin. A dual quaternion solution to attitude and position control for rigid-body coordination. *IEEE Trans. Robot.*, 28(5):1162–1170, 2012.

J.T.-Y. Wen and K. Kreutz-Delgado. The attitude control problem. *IEEE Trans. Autom. Control*, 36(10):1148–1162, 1991.

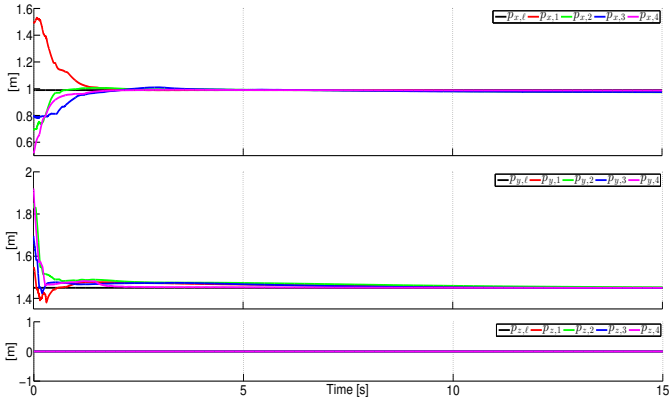

Fig. 1. Robots position.

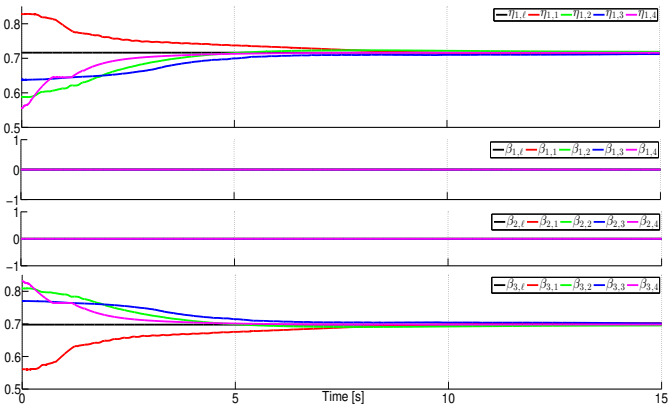

Fig. 2. Robots quaternion orientation.

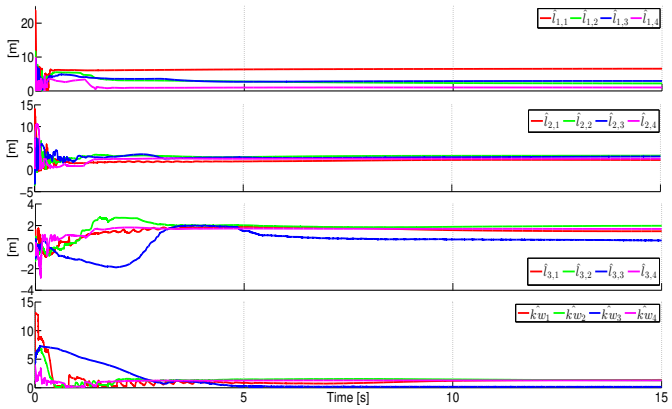

Fig. 3. Kinematic parameters estimation.